Journal of Renewable Materials

Tech Science Press

DOI: 10.32604/jrm.2024.047758

ARTICLE

Performance Analysis of Plant Shells/PVC Composites under Corrosion and Aging Conditions

Haoping Yao[1], Xinyu Zhong[2] and Chunxia He[1,*]

[1]College of Engineering, Nanjing Agricultural University, Nanjing, 210031, China

[2]School of Mechanical Engineering, Shanghai Jiao Tong University, Shanghai, 200240, China

[*]Corresponding Author: Chunxia He. Email: chunxiahe@njau.edu.cn

Received: 16 November 2023 Accepted: 06 May 2024 Published: 17 July 2024

ABSTRACT

To make full use of plant shell fibers (rice husk, walnut shell, chestnut shell), three kinds of wood-plastic composites of plant shell fibers and polyvinyl chloride (PVC) were prepared. X-ray diffraction analysis was carried out on three kinds of plant shell fibers to test their crystallinity. The aging process of the composites was conducted under 2 different conditions. One was artificial seawater immersion and xenon lamp irradiation, and the other one was deionized water spray and xenon lamp irradiation. The mechanical properties (tensile strength, flexural strength, impact strength), changes in color, water absorption, Fourier transform infrared spectroscopy (FTIR), and microstructures of the composites before and after the two aging experiments were analyzed. The results showed that the chestnut shell had the highest crystallinity, which was 42%. The chestnut shell/PVC composites had the strongest interface bonding, the least internal defects, and the best general mechanical properties among the three composites. Its tensile strength, bending strength and impact strength were 23.81 MPa, 34.12 MPa, and 4.32 KJ·m^{-2}, respectively. Comparing the two aging conditions, artificial seawater immersion and xenon lamp irradiation destroyed the quality of the combination of plant shell fibers and PVC, making the internal defects of the composites increase. This made the water absorption ability and changes in the color of the composites more obvious and led to a great decrease in the mechanical properties. The general mechanical properties of the chestnut shell/PVC composites were the best, but their water absorption ability changed more obviously.

KEYWORDS

Plant shell fibers; polyvinyl chloride; wood-plastic composites; artificial seawater immersion; deionized water spray; xenon lamp irradiation

1 Introduction

Wood-plastic composites (WPCs) are made of plant fiber and plastic via proper processing methods such as hot pressing and melt extrusion. They are environmentally friendly and not only have the toughness and processability of plastics, but also have the hardness of wood [1–3]. They are often used in building materials, outdoor facilities, forest construction, packaging boxes, transportation facilities, etc. [4–7]. However, plastics are prone to aging if exposed to sunlight, and plant fibers are prone to corrosion if exposed to corrosive solutions. Both phenomena will lead to a decline in the performance of WPCs [8–11]. Nowadays, the application of WPCs in commercial fields and marine environments is increasing.

When they are placed outdoors, their performance will decline and their internal structure will be damaged, such as matrix plasticization, surface foaming, etc. [12–14]. Therefore, it is important to study the UV aging resistance and corrosion resistance of WPCs.

There has been some research on the impact of seawater or ultraviolet environment on the performance of WPCs. The effects of the Caspian Sea and Persian Gulf Sea water on the water absorption and bending properties of Wood-Polypropylene (PP) composites were studied by Saeed KN et al. [15]. The results showed that the influence of seawater on the physical and mechanical properties of WPCs was closely related to seawater salinity and plant fiber content. The effects of natural weathering on the physical and mechanical properties of biodegradable composites based on poly (3-hydroxybutyrate-*co*-3-hydroxyvalerate) (PHBV) and wood flour (WF) were studied. The results showed that over a period of 12 months, 20% of the WF samples had little loss in mechanical properties [16]. The wear behavior of WPCs exposed to simulated seawater and acid rain by turns was studied by Jiang et al. The results showed that the salinity and temperature of seawater, as well as the pH value and temperature of acid rain, would reduce the wear resistance, hardness, and tensile strength of WPCs [17]. The influences of the plastic matrix (HDPE, HDPE, PP, PVC, and PS) on mechanical properties (flexural and tensile properties) of wood-plastic composites (WPCs) after aging 2160 h were investigated. The results indicated that the WPCs with PS and PP had the smallest losses of mechanical properties after aging, while LDPE would be the poorest choice in this respect [18]. The degradation of the four wood dust (Babool, Sheesham, Mango, and Mahogany trees)/Polypropylene (PP) composites due to Ultraviolet-B (UVB) radiation were studied by Vedrtnam et al. The results showed that the UVB radiation exposure deteriorates the matrix of WPCs which results in inferior mechanical properties [19].

When WPCs are used in coastal areas, they are exposed to the combined effects of seawater corrosion and sunlight aging, thus reducing the bonding quality between fibers and matrix and deteriorating the service performance of WPCs. In the field of shell plant fiber-reinforced WPCs, research on rice husk-reinforced WPCs has received more attention than walnut shell and chestnut shell-reinforced WPCs. Therefore, in this study, the performance of composites prepared by three different plant shell fibers (rice husk, walnut shell, chestnut shell) and PVC were studied under two aging experiments. One experiment was artificial seawater immersion and xenon lamp irradiation, and another one was deionized water spray and xenon lamp irradiation. The corrosion and aging mechanism of three kinds of composites were discussed and analyzed.

2 Materials and Methods

2.1 Materials

Rice husk powder, walnut shell powder and chestnut shell powder were produced in Lianyungang, Jiangsu, all of which were 100 mesh. PVC (100 mesh) and calcium-zinc stabilizer were purchased from Shaoyang Tiantang Auxiliary Co., Ltd. (Shaoyang, China). Male-grafted PVC was purchased from LG Company in Korea and PE wax (SQI-H108) was purchased from Thailand SQI Company.

2.2 Sample Preparation

The plant shell powder was dried at 90°C for 12 h. Then they were filtered with a 100-mesh sieve. The ratio between different plant shell powder:PVC:calcium zinc stabilizer:PE wax:male-grafted PVC was adjusted to 100:100:8:5:3.

The mixed materials were put into the RM200C conical twin-screw base platform and extruded to obtain three kinds of WPCs. The working parameters of the twin-screw extruder were set as follows. The temperatures in the four zones were 150°C, 155°C, 160°C, and 165°C, respectively, and the pressure of the head was 0.5 MPa. After demolding, the composites were cut into strips with a width of about 7 cm and a height of about 10 cm according to the test standard.

2.3 Two Kinds of Corrosion and Aging Experiments

2.3.1 Artificial Seawater Immersion and Xenon Lamp Irradiation

The composites were immersed into artificial seawater and were then put into a xenon lamp aging test box with a temperature set at 60 ± 1°C. The treatment was set with the illumination time of 100 min with an interval of 20 min, and kept cycling. During the experiment, the composites was continuously immersed into artificial seawater. The treatment time was 72, 144, and 216 h.

Artificial seawater was prepared according to the literature [20]. Deionized water was used as the solvent, and the content of artificial seawater was NaCl (26.5 $g{\cdot}L^{-1}$), $MgCl_2$ (24 $g{\cdot}L^{-1}$), $CaCl_2$ (1.1 $g{\cdot}L^{-1}$), $MgSO_4$ (3.3 $g{\cdot}L^{-1}$), $NaHCO_3$ (0.2 $g{\cdot}L^{-1}$), KCl (0.73 $g{\cdot}L^{-1}$), and NaBr (0.28 $g{\cdot}L^{-1}$). To make the artificial seawater slightly alkaline, an appropriate amount of NaOH was added to the prepared solution.

2.3.2 Deionized Water Spray and Xenon Lamp Irradiation

The composites were put into xenon lamp aging test box, the temperature was kept at 60 ± 1°C. The treatment was set with the illumination time for 100 min with an interval of 20 min. At the same time, the composites were sprayed with deionized water during dark time. The treatment time was the same as that of the artificial seawater and xenon lamp irradiation aging test.

In the following, the deionized water spray and xenon lamp irradiation corrosion aging experiment was set as treatment I, and artificial seawater immersion and xenon lamp irradiation corrosion aging experiment was set as treatment II.

2.4 Performance Test

2.4.1 Mechanical Properties

According to standards (Standardization Administration of the People's Republic of China, Determination of tensile properties of plastics: GB/T 1040.1–2006 and Determination of flexural properties of plastics: GB/T 9341–2008), the tensile strength and bending strength of composites were tested. The impact strength of composites was tested according to the standards (Determination of charpy impact properties of plastics: GB/T 1043.1–2008). Each test was done three times, and the results were averaged.

2.4.2 Water Absorption Rate

According to standards (Test method for water absorption of fiber reinforced plastic: GB/T 1462-2005), the dried composite samples were put into an HH-600 digital display constant temperature water box, and the temperature was kept at 35 ± 1°C. The average of three tests was taken as the result.

2.4.3 Color Difference

According to the CIE 1976L*a*b colorimetric system, the color change of the composite surface before and after the experiment was tested using HP-200 precision colorimeter (Shanghai Hanpu Optoelectronics Technology Co., Ltd., Shanghai, China). Each sample was tested 6 times at different locations, and the average values were taken. The color difference was calculated according to formula (1).

$$\Delta E = \sqrt{(\Delta L)^2 + (\Delta A)^2 + (\Delta B)^2} \tag{1}$$

ΔE is the color difference. L is the lightness coordinate, ranging from 0 to 100. When ΔL is a positive value, it means that the composites are white, and a negative value means that they are black. A is the chromaticity coordinates of red to green, ranging from −150 to +150. When ΔA is positive, the composites are red, and a negative value represents green. B represents the chromaticity coordinates of yellow to blue, ranging from −150 to +150. When ΔB is positive, the composites turn yellow, and a negative value means blue.

2.4.4 Infrared Spectroscopy

The chemical surface functional groups of the composites were tested using a NicoletiS-10 Fourier transform infrared (FTIR) spectrometer (Dumei Precision Instrument Co., Ltd., Shanghai, China). The samples after grinding and tableting were scanned 16 times with a resolution of 4 cm^{-1} and scanning wave numbers from 4000 to 400 cm^{-1}.

2.4.5 X-ray Diffraction

The crystallinity of three kinds of plant shell powders was tested by X'Pert PRO X-ray diffractometer (XRD, Analytical B.V., Almelo, Netherlands), with a Cu K α radiation source (λ = 1.54056) and scanning range from 10° to 90°. Calculated the crystallinity according to formula (2):

$$Crl = \left(1 - \frac{I_{am}}{I_{002}}\right) \times 100\% \tag{2}$$

where Crl is the degree of crystallinity, I_{am} is the strength of the amorphous phase, and I_{002} is the strength of the crystalline phase.

2.4.6 Microstructure

After gold-spraying on the tensile sections of the composites, the surface microstructures of the composites were performed using an S-4800 scanning electron microscope (SEM, Hitachi, Ltd., Tokyo, Japan).

3 Results and Discussion

3.1 Crystallinity Analysis of the Plant Shell Fibers

Fig. 1 shows the XRD patterns of the three kinds of plant shell fibers. There were peaks in the XRD patterns of different fibers when 2θ was 16° and 22°, but the intensities of the peaks were different. The peak at 2θ = 16° is related to lignin and hemicellulose, and 2θ = 22° is related to cellulose molecules [21].

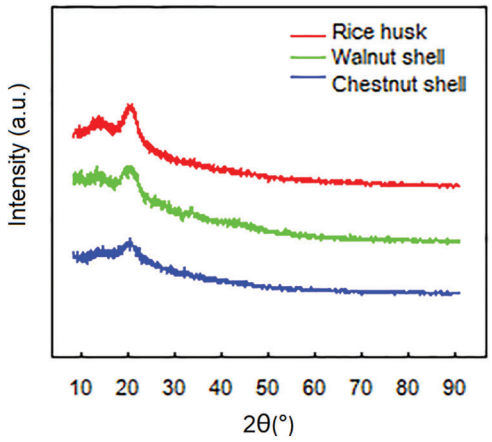

Figure 1: XRD maps of the three plant shell fibers

The crystallinity of three plant shell fibers calculated by formula (2) is shown in Table 1. The crystallinity of chestnut shell fiber was 42%, which was much higher than that of rice husk and walnut shell fiber, and the crystallinity of walnut shell fiber was the lowest, which was 25.4%. The differences in chemical compositions and structures of plant fibers lead to different crystallinity. Cellulose in plant fibers is a crystalline phase, and the proportion of cellulose in plant fibers with high crystallinity is also higher. The cellulose contents of chestnut shell, rice husk and walnut shell fibers are 47.96%, 34.72% and 30.88%, respectively [22–24], which is consistent with the crystallinity of the plant fibers. The molecular arrangement in cellulose is regular, and the reactivity of hydroxyl is much lower than that of hydroxyl in

the amorphous phase. The higher the crystallinity of the plant fiber, the lower the active hydroxyl group content in the fiber, so for the surface polarity of the fiber. This makes the interfacial strength between the PVC and the fiber higher and the internal defects of the composites less [24]. The crystallinity of plant fibers has a positive impact on the mechanical properties, water absorption and anti-corrosion and aging properties of the composites.

Table 1: Crystallinity of three plant shell fibers

Plant shell fiber type	Rice husk	Walnut shell	Chestnut shell
Crystallinity (%)	26.1	25.4	42

3.2 Mechanical Properties Analysis of the Composites

Figs. 2 and 3 show the mechanical properties of three kinds of plant shell fiber/PVC composites before and after 2 treatments. Before treatment, the chestnut shell/PVC composites had the best mechanical properties; its tensile strength was 23.81 MPa, the bending strength was 34.12 MPa and impact strength was 4.32 KJ·m^{-2}. The walnut shell/PVC composites had the worst general mechanical properties; their tensile strength was 18.33 MPa, bending strength was 30.98 MPa and impact strength was 3.78 KJ·m^{-2}. After 2 treatments, the mechanical properties of the three composites showed different degrees of decline. And the longer the corrosion aging time, the more the mechanical properties decrease. Overall, the properties of the chestnut shell/PVC composites had less loss. Its tensile strength, flexural strength, and impact strength were lost by 21.82%, 27.07% and 34.72% respectively under treatment I. Under the treatment II, these properties were lost by 27.28%, 37.62% and 41.67%, respectively. The general mechanical properties of walnut shell/PVC composites decreased significantly. Comparing the decrease under the two aging methods, treatment II made the mechanical properties of the composites decrease more.

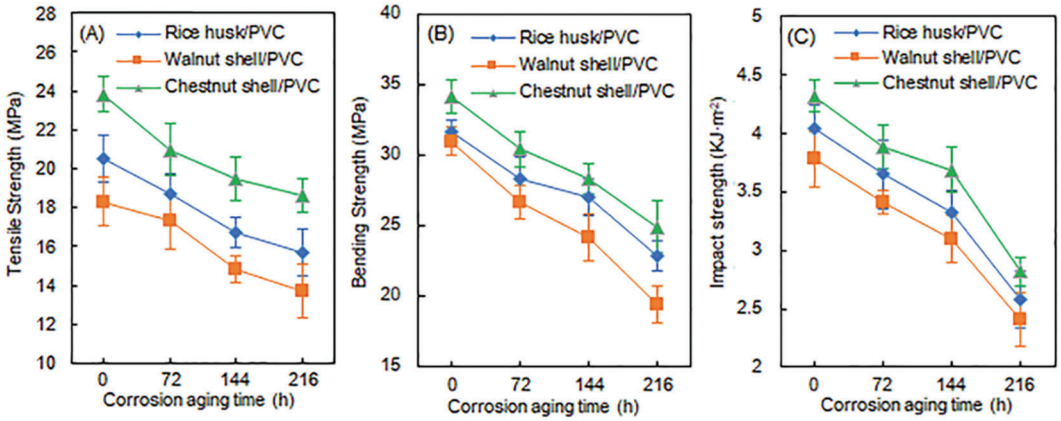

Figure 2: Tensile strength (A), bending strength (B) and impact strength (C) of the composites under treatment I

Comparing the performance of composites under the two treatments, the mechanical properties of the composites decreased more obviously under treatment II. The reason is that xenon lamp aging and seawater corrosion promote each other. The chemical bonds of PVC molecular chains are broken and degraded by ultraviolet rays from xenon lamps [25]. At the same time, ultraviolet rays cause the photodegradation of hemicellulose. These reduce the mechanical association and the molecular attraction between the shell fibers and PVC matrix, and aggravate the generation of cracks. NaCl, $MgCl_2$, KCl and other components in artificial seawater enter the composites. This leads to a large amount of salt

presenting at the connection of the shell fibers and the matrix after drying the composites, which increases the free volume of the composites, makes the molecular chain movement more free, and makes the shell fibers contact with seawater more frequently. Due to the influence of artificial seawater, the shell fiber easily absorbs water and swells to crack the PVC coating on the outside, resulting in many cracks on the junction of the shell fibers and the matrix. Under the action of external force, the defects of composites were prone to stress concentration and fracture damage. In addition, artificial seawater has a plasticizing effect on composites, which can increase the freedom of fiber molecules in plant shell fibers and weaken the rigidity of the composites [17]. The composites were mainly subjected to light aging under treatment I. After the reaction, the shell fibers did not separate from the composites, there were some cracks on the junction of the fibers and the PVC.

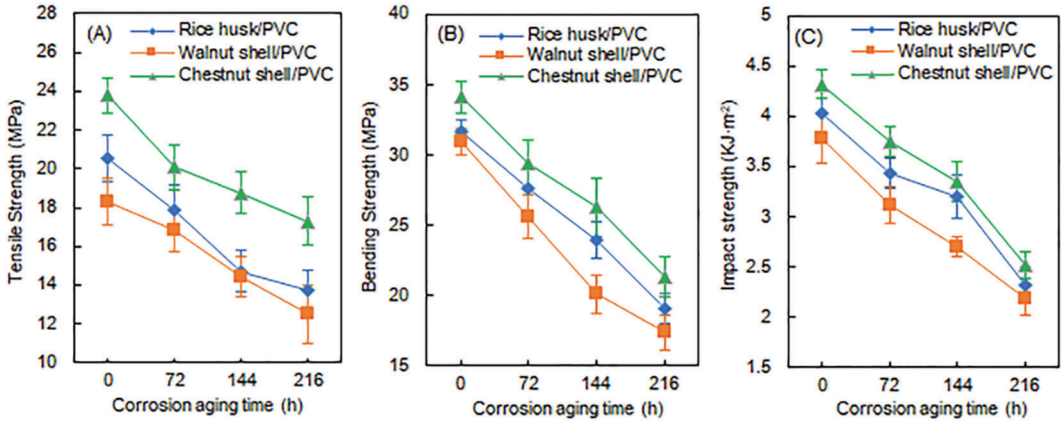

Figure 3: Tensile strength (A), bending strength (B) and impact strength (C) of the composites under treatment II

3.3 FTIR Analysis of the Composites

Fig. 4 is the infrared spectrum of the composites. The FTIR spectra of the three composites after corrosion and aging mainly changed in the location of the absorption peak. Within the 3200–3400 cm^{-1} sband, it corresponds to hydroxyl vibration, which mainly comes from cellulose. After corrosion and aging, the peaks of the three composites increased within this band, indicating the increase in the content of hydroxyl groups. The reason is that the surface bonding quality of plant shell fibers and PVC matrix decreases, and more plant shell fibers are exposed after corrosion and aging, resulting in an increase in the hydroxyl content in the composites. The peak change under treatment II was more significant than that under treatment I, indicating that it was more destructive to the composites. The peaks around 1700 cm^{-1} changed obviously after corrosion aging; the non-conjugated carbonyl group corresponding to 1734 cm^{-1} and the conjugated carbonyl group corresponding to 1637 cm^{-1} increased significantly. The reason is that the aromatic structure (chromophore) of lignin absorbs ultraviolet light, and the chromophore is degraded to produce a carboxyl group and a carbonyl group under photo-oxidation. The reason for the increase of the conjugated carbonyl group is the breakage of the β-O bond in lignin, resulting in the appearance of a quinoid on the aromatic ring. In the preparation of composites, plant fibers and the carbonyl groups of PVC are bound to the PVC matrix. Under the action of ultraviolet light, the composites absorb incident light and initiate a dehydrochlorination reaction, resulting in the photodegradation of the composites [26]. Under treatment II, the surface bonding quality of the composites deteriorated significantly, and the photodegradation was stronger than that under treatment I. Cellulose oxides and hydroperoxides generated from cellulose reacting with oxygen decomposed to form ketone groups that enhanced the peak of carbonyl groups. Therefore, the increase of the carbonyl groups

indicated the deepening of the oxidative degradation of the composites. The peak was strengthened in the 1400–1500 cm^{-1} band, which showed that the stretching vibration of methyl and methylene in PVC was strengthened. The reason is that in the process of corrosion and aging, the PVC matrix of the composites is degraded, and the molecular chain breakage causes the CH_3- and -CH_2- content to increase [17]. The absorption peaks at 1375 cm^{-1} and 1163 cm^{-1} corresponded to the fragmentation of CH and C-O-C, respectively. The peak at 1103 cm^{-1} corresponded to a partial β-(1,4)-glycosidic bond cleavage in cellulose. These all showed that the composites have degraded.

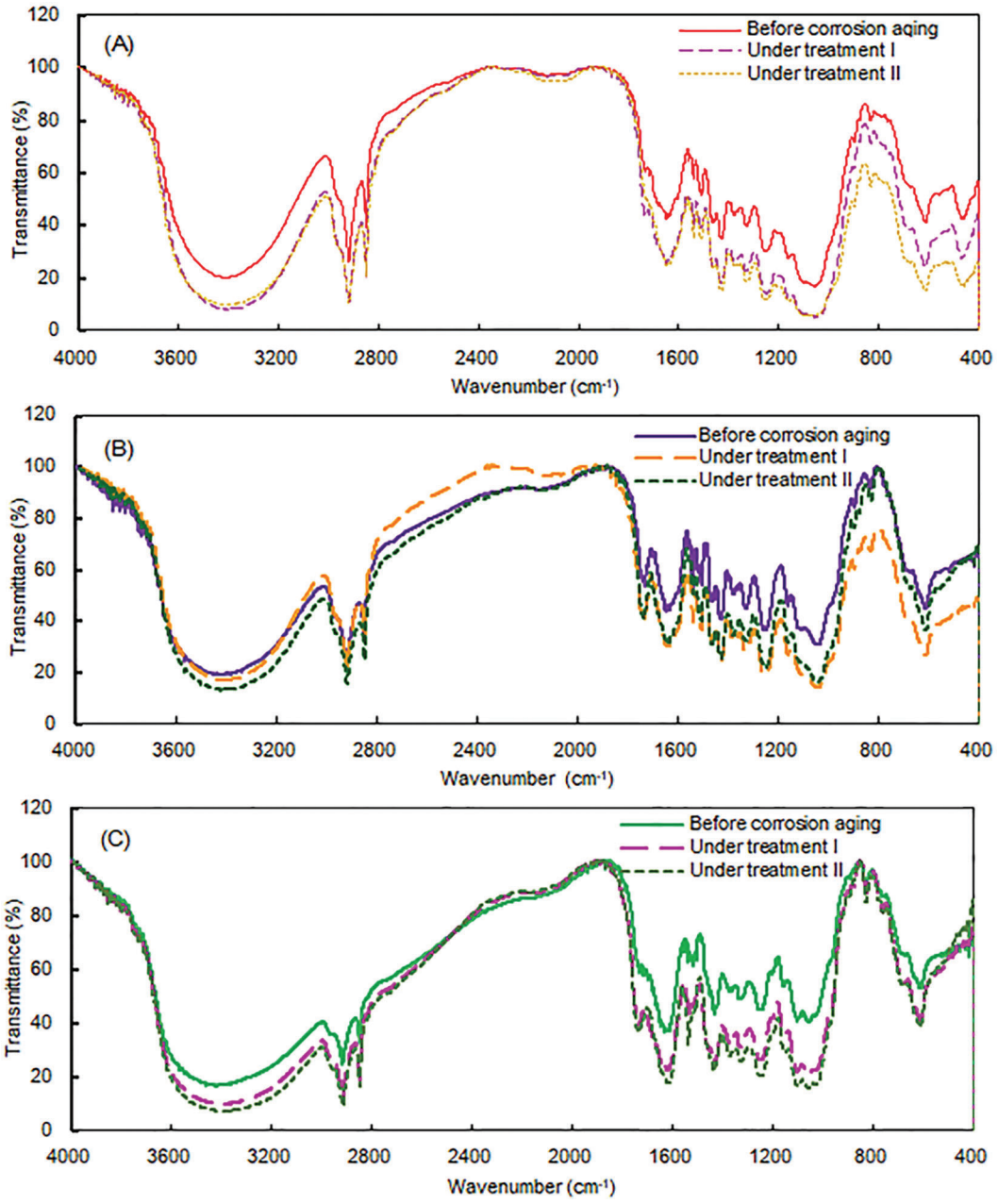

Figure 4: FTIR spectra of the composites. (A) rice husk/PVC, (B) walnut shell/PVC and (C) chestnut shell/PVC

3.4 Micro-Interface Structure Analysis of the Composites

Figs. 5–7 show the microstructure of the composites before and after 2 treatments. In Fig. 5, the chestnut shell/PVC composites had the best interfacial compatibility, and the combination of the two phases was tight with only a few defects such as gaps and voids before corrosion and aging. The interfacial compatibility of rice husk/PVC composites was relatively poor, and there were some small gaps. According to the analysis of the crystallinity of plant shell fibers in Section 3.1, among the three kinds of plant shell fibers, chestnut shell fibers had the highest crystallinity, relatively high cellulose content, and relatively low surface polarity, and the plant fibers were closely combined with PVC. Within a certain range of cellulose content, the increase of cellulose content can lead to an increase in mechanical properties and fiber-matrix adhesion, and the interfacial compatibility between the fiber and matrix is better [27]. The interface between fibers and PVC in composites controls the stress transfer between them. In the process of the composites forming, PVC infiltrates the uneven parts on the surface of plant fibers like peaks, holes, cracks, etc., and mechanically locks on the plant fibers via adhesion. Then the relative movement between the fibers and the matrix is limited. Therefore, good stress transfer and mechanical action were maintained between the two phases [28]. The surface shape of chestnut shell fibers was irregular, and the strong mechanical interaction with PVC led to good mechanical properties of the composites, which was consistent with the results in Section 3.2.

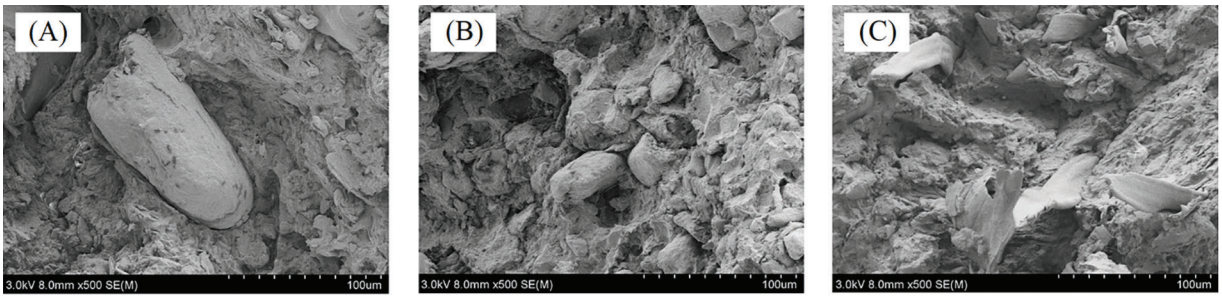

Figure 5: Micromorphology of the composites before corrosion aging. (A) rice husk/PVC, (B) walnut shell/PVC and (C) chestnut shell/PVC

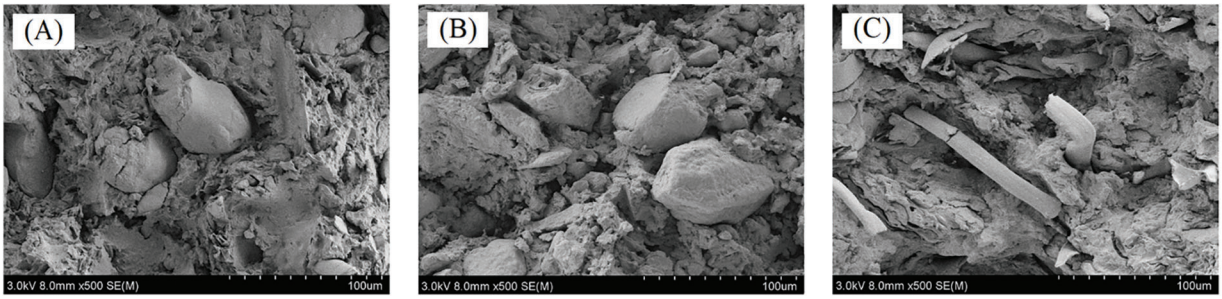

Figure 6: Micro-morphology of the composites under treatment I. (A) rice husk/PVC, (B) walnut shell/PVC and (C) chestnut shell/PVC

In Figs. 6 and 7, after 2 treatments, the internal defects of the three composites increased significantly, and many cracks and holes appeared in their cross-sections. Plant fibers were exposed to the outside without being wrapped in PVC. Comparing the composites after 2 treatments, in the composites under treatment II, not only did the fibers peel off from the matrix, leaving more voids, but also the microcracks in the bonding face between fibers and PVC increased. The reason is that xenon lamp aging and seawater corrosion can reduce the quality of the two phases and increase the number of cracks. In addition, the fibers absorbed

water and expanded. Then the fibers are exposed to the external environment, causing the larger gaps between the two phases. Part of the exposed plant fibers peel off, resulting in the deepening of the artificial seawater color after soaking the composites. However, the composites only undergo photochemical reactions under treatment I, which deteriorates the bonding quality of the composites and increases the number of cracks. However, the fiber and the PVC are still connected together. The degree of deterioration of the composites is relatively small. Comparing the micro-morphologies of the three composites after corrosion and aging, the chestnut shell/PVC composites had fewer defects and better material performance. This is consistent with the conclusion in Section 3.1 that the higher the crystallinity of the chestnut shell fiber, the higher the interfacial strength between the matrix and the plant fibers, and the fewer the internal defects of the composites.

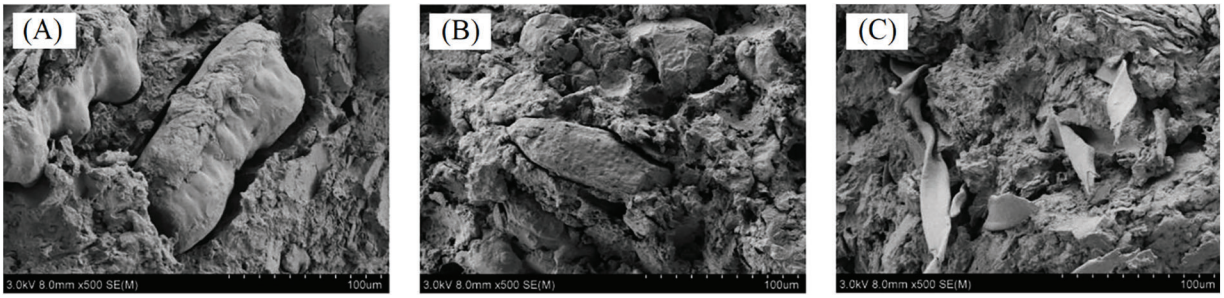

Figure 7: Micro-morphology of the composites under treatment II. (A) rice husk/PVC, (B) walnut shell/PVC and (C) chestnut shell/PVC

3.5 Color Difference Analysis of the Composites

Tables 2 and 3 show the color difference changes of three kinds of plant shell fiber/PVC composites under 2 treatments. With the increase of corrosion aging time, the ΔE value of the three composites increased continuously, indicating the increase of change of color difference. According to formula (1), the ΔL, ΔA and ΔB have an impact on ΔE, but the decisive role is ΔL. So, the determining factor for the color change of composites is brightness. After treatments, the three composites had obvious fading. When ΔE exceeds 12, the human visual perception will be obvious. In the test, the ΔE's were all above 20, and the surface color changes (mainly whitening) of the three composites were obvious and the degree of fading gradually increased.

Table 2: Variation of color difference of the composites under treatment I

Composites	Processing hours/h					
	72		144		216	
Rice husk/PVC composites	ΔL	23.14 ± 1.38	ΔL	22.4367 ± 1.7	ΔL	26.93 ± 1.91
	ΔA	0.35 ± 0.55	ΔA	0.07 ± 0.3	ΔA	−1.6233 ± 0.23
	ΔB	0.6967 ± 0.36	ΔB	0.0167 ± 0.77	ΔB	−4.17 ± 0.79
	ΔE	23.1639 ± 1.35	ΔE	22.4515 ± 1.71	ΔE	27.3044 ± 2.01
Walnut shell/PVC composites	ΔL	27.3067 ± 1.3	ΔL	37.81 ± 0.4	ΔL	36.3167 ± 1.99
	ΔA	1.1033 ± 0.1	ΔA	1.22 ± 0.2	ΔA	0.1267 ± 0.36
	ΔB	−2.84 ± 0.59	ΔB	−0.59 ± 0.22	ΔB	−3.19 ± 0.34
	ΔE	27.4845 ± 1.26	ΔE	37.8354 ± 0.4	ΔE	36.4591 ± 2.01

(Continued)

Table 2 (continued)

Composites	Processing hours/h					
	72		144		216	
Chestnut shell/PVC composites	ΔL	12.2067 ± 4.45	ΔL	16.1233 ± 0.75	ΔL	19.8667 ± 2.63
	ΔA	9.5967 ± 3.5	ΔA	12.39 ± 0.93	ΔA	11.2133 ± 0.65
	ΔB	5.68 ± 2.7	ΔB	10.31 ± 0.45	ΔB	8.38 ± 0.95
	ΔE	17.646 ± 1.16	ΔE	22.8057 ± 1.15	ΔE	24.4177 ± 1.63

Table 3: Variation of the color difference of the composites under treatment II

Composites	Processing hours/h					
	72		144		216	
Rice husk/PVC composites	ΔL	30.5267 ± 1.18	ΔL	33.9 ± 4.52	ΔL	33.62 ± 1.49
	ΔA	0.6867 ± 0.15	ΔA	0.2167 ± 0.1	ΔA	−0.57 ± 0.23
	ΔB	0.1333 ± 0.28	ΔB	−1.0467 ± 0.53	ΔB	−0.6 ± 0.27
	ΔE	30.5361 ± 1.19	ΔE	33.9255 ± 4.51	ΔE	33.6323 ± 1.48
Walnut shell/PVC composites	ΔL	20.4367 ± 1.28	ΔL	21.4667 ± 2.88	ΔL	38.1 ± 10.98
	ΔA	1.3833 ± 0.56	ΔA	1.91 ± 0.99	ΔA	0.8933 ± 1.95
	ΔB	−0.11 ± 0.88	ΔB	−0.1067 ± 0.78	ΔB	−1.3367 ± 1.55
	ΔE	20.5088 ± 1.3	ΔE	21.6055 ± 2.75	ΔE	38.2463 ± 10.86
Chestnut shell/PVC composites	ΔL	12.0233 ± 5.26	ΔL	22.4067 ± 0.62	ΔL	31.6333 ± 1.28
	ΔA	15.1767 ± 2.58	ΔA	11.6633 ± 0.22	ΔA	7.0367 ± 0.25
	ΔB	9.45 ± 1.65	ΔB	6.3833 ± 0.71	ΔB	6.4433 ± 0.49
	ΔE	22.3625 ± 1.09	ΔE	26.0705 ± 0.34	ΔE	33.0527 ± 1.08

After 216 h of treatment, the color of the walnut shell/PVC composites changed the most. The ΔE values under treatment I and treatment II were 36.4591 and 38.246, respectively. Photo-oxidation of lignin in wood led to changes in the surface color of the composites, and the UV absorbed by lignin accounts for 80%–95% of the wood. The oxidation of lignin formed a p-benzoquinone chromophore structure, causing the composites to turn yellow. At the same time, p-benzoquinone is reduced to form hydroquinone, causing the composites to undergo photofading. The lignin content in the walnut shell among the three kinds of plant shell fibers is the highest at 38.05%, which leads to the largest color change of the composites [17]. After 216 h of corrosion and aging, the color change of the chestnut shell/PVC composites was the smallest. The ΔE values under treatment I and treatment II were 24.4177 and 33.0527, respectively.

Under 2 treatments, the color of the composites changed significantly. The reason is that under the action of UV, the matrix is photo-oxidized and decomposed, generating the chemical transformation structure of polyene and oxygen-containing groups [29]. This causes the change in the strength and color of the composites. Photochemical reactions and chromatic aberration in composites also lead to the formation of aromatic and other free radicals, resulting in the degradation of lignin and photo-oxidation of cellulose

and hemicellulose, thus causing color differences. Comparing the composites under 2 treatments, the color change of the composites under treatment II was more obvious. The reason is that many defects are formed inside the composites due to artificial seawater corrosion, and the contact of artificial seawater with the plant shell fibers detached from the PVC coating causes the pigments in the fibers to dissolve in the seawater, resulting in significant changes in the color of the composites [30]. In Fig. 4, the carbonyl stretching vibration and the stretching vibration of the carbon-carbon bond of the benzene ring of the composites were significantly strengthened in the 1500–1700 cm^{-1} band and the 1450–1600 cm^{-1} band. So, under 2 treatments, photochemical reactions occurred to generate chromophoric groups, promoting the color change of the composites.

3.6 Water Absorption Analysis of the Composites

According to Fig. 8, with the increase in corrosion aging time, the water absorption of the three composites had an increasing trend. The water absorption rate of rice husk/PVC composites was the lowest, and the water absorption rates under treatment I and treatment II for 216 h were 3.01% and 3.22% respectively. The water absorption rate of chestnut shell/PVC composites was the highest, and the water absorption rate under 2 treatments for 216 h were 3.67% and 4.05%, respectively. Comparing Fig. 8A,B, the water absorption rates of the three composites under treatment II were higher than those under treatment I. The reason is that the combined action of artificial seawater and xenon lamp leads to complex reactions in the composites, such as photo-oxidation, corrosion, etc., which makes the matrix degrade and the fiber loss. In addition, due to the different surface polarity between the fibers and matrix, the defects in the joint surface such as cracks are further enlarged, making the hydrophilic group in the plant shell fibers more likely to come into contact with water. The degree of deterioration and internal defects of the composites under treatment II were more serious than those under treatment I, which was consistent with the characteristics of the micro-morphology of the composites after corrosion and aging in Figs. 6 and 7.

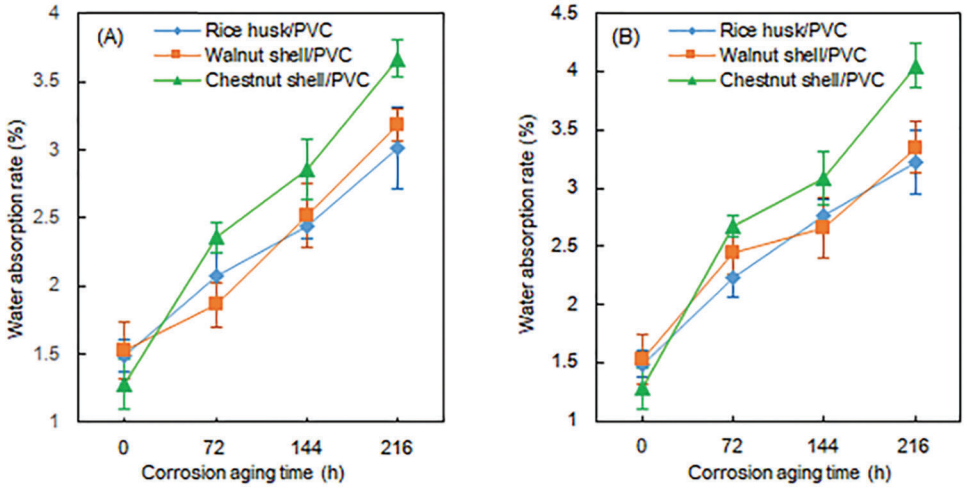

Figure 8: Water absorption of the composites. (A) under treatment I, (B) under treatment II

In Fig. 8, before corrosion and aging, the water absorption rate of the chestnut shell/PVC composites was the lowest. The reason is that the chestnut shell has a high degree of crystallinity, the hydrophilic hydroxyl groups contained in it are linked to each other, and the content of free hydroxyl groups is relatively low. Therefore, it shows a low polarity, and it is tightly attached to matrix, making it difficult to meet water molecules. After corrosion and aging, the chestnut shell/PVC composite has the largest

variation in water absorption, becoming the highest one among the three composites. Due to the relatively high content of cellulose and hemicellulose in the chestnut shell, many fibers were exposed to the outside of PVC after corrosion and aging, which led to the recovery of the polarity of the plant fibers itself and made the water absorption rate of the composites change most obviously.

4 Conclusion

(1) Among the three composites, the general mechanical properties of chestnut shell/PVC composites were the best, while those of walnut shell/PVC composites were the poorest. After corrosion and aging, the properties of chestnut shell/PVC composites decreased slightly, while those of walnut shell/PVC composites decreased the most. Comparing the two corrosion aging methods, the mechanical properties of the composites under treatment II were greatly reduced.

(2) After the corrosion and aging of the 2 treatments, the color of the three composites was changed. The composites under treatment II had the most obvious color change. In this treatment, the ΔE value of the chestnut shell/PVC composites was the smallest, and its ΔE value was 33.05, while the ΔE value of the walnut shell/PVC composite was the largest, which was 38.2. In addition, the water absorption rate of the composite increased after corrosion and aging, and that of the chestnut shell/PVC composite changed the most.

(3) Under treatment II, the structures of the three composites deteriorated to varying degrees, and defects such as cracks and holes were generated. The bonding quality between the two phases decreased. The chestnut shell fibers had high crystallinity, low content of active hydroxyl groups, and were more closely combined with the PVC matrix. They also had fewer internal defects than the other composites. Therefore, the composites formed by it had the best general performance before and after corrosion and aging.

Acknowledgement: The authors would like to thank the Key Laboratory of Intelligence Agricultural Equipment of Jiangsu Province, which provided the facilities for the experiment.

Funding Statement: This study was supported by the financial support of Natural Science Research Projects in Higher Education Institutions in Jiangsu Province (No. 18KJD430002).

Author Contributions: Study conception and design: Chunxia He, Haoping Yao, Xinyu Zhong; data collection: Haoping Yao, Xinyu Zhong; analysis and interpretation of results: Haoping Yao, Xinyu Zhong; draft manuscript preparation: Chunxia He, Haoping Yao, Xinyu Zhong. All authors reviewed the results and approved the final version of the manuscript.

Availability of Data and Materials: The data is available on request from the authors.

Conflicts of Interest: The authors declare that they have no conflicts of interest to report regarding the present study.

References

1. Issam E, Fethi A, Mohamed H, Furqan A, Mohamed G, Mondher N, et al. A comprehensive review of natural fibers and their composites: an eco-friendly alternative to conventional materials. Results Eng. 2023;19:101271. doi:10.1016/j.rineng.2023.101271.
2. Bijlwan PP, Prasad L, Sharma A. Recent advancement in the fabrication and characterization of natural fiber reinforced composite: a review. Mater Today. 2021;44(1):1718–22.
3. Ayyappan V, Mavinkere RS, Siengchin S, Parameswaranpillai J. Renewable and sustainable biobased materials: an assessment on biofibers, biofilms, biopolymers and biocomposites. J Clean Prod. 2022;258:120978.

4. Mohammed M, Anwar JMJ, Aeshah MM, Jawad KO, Tijjani A, Azlin FO, et al. Challenges and advancement in water absorption of natural fiber-reinforced polymer composites. Polym Test. 2023;124:108083.
5. Yang SQ, Wei BJ, Wang Q. Superior dispersion led excellent performance of wood—plastic composites via solid —state shear milling process. Compos Part B. 2020;200(16):108347.
6. Habibi M, Selmi S, Laperrière L, Mahi H, Kelouwani S. Post-impact compression behavior of natural flax fiber composites. J Nat Fibers. 2020;17(11):1683–91. doi:10.1080/15440478.2019.1588829.
7. Daniel F. Thermoplastic moulding of wood-polymer composites (WPC): a review on physical and mechanical behaviour under hot-pressing technique. Compos Struct. 2021;262(5):113649.
8. Yaguchi Y, Takeuchi K, Waragai T, Tateno T. Durability evaluation of an additive manufactured biodegradable composite with continuous natural fiber in various conditions reproducing usage environment. Int J Auto Tech-JPN. 2020;14(6):959–65. doi:10.20965/ijat.2020.p0959.
9. Kychkin AK, Startsev OV, Lebedev MP, Polyakov VV. Effect of solar radiation and synergism of the effect of UV radiation, temperature and moisture on the distraction of polymer composite materials in a cold climate. Proc Struct. 2020;30:71–5.
10. Awaja F, Zhang S, Tripathi M, Nikiforov A, Pugno N. Cracks, microcracks and fracture in polymer structures: formation, detection, autonomic repair. Prog Mater Sci. 2016;83:536–73. doi:10.1016/j.pmatsci.2016.07.007.
11. Vercher J, Fombuena V, Diaz A, Soriano M. Influence of fibre and matrix characteristics on properties and durability of wood-plastic composites in outdoor applications. J Thermoplast Compos. 2020;33(4):477–500. doi:10.1177/0892705718807956.
12. Jiang LP, Fu JJ, He CX. Reliability analysis of wood-plastic composites in simulated seawater conditions: effect of iron oxide pigments. J Build Eng. 2020;31:101138.
13. Kuka E, Andersons B, Cirule D, Andersone I, Kajaks J, Militz H, et al. Weathering properties of wood-plastic composites based on heat-treated wood and polypropylene. Compos Part A: Appli Sci Manufactur. 2020;139:106102. doi:10.1016/j.compositesa.2020.106102.
14. Segovia F, Salvador MD, Sahuquillo O, Vicente A. Effects of long-term exposure on e-glass composite material subjected to stress corrosion in a saline medium. J Compos Mater. 2007;41(17):2119–28.
15. Saeed KN, Hamed YK. Effect of sea water on water absorption and flexural properties. Eur J Wood Prod. 2011;69:553–6. doi:10.1007/s00107-010-0518-7.
16. Chan CM, Pratt S, Halley P, Richardson M, Werker A, Laycock B, et al. Mechanical and physical stability of polyhydroxyalkanoate (PHA)-based wood plastic composites (WPCs) under natural weathering. Polym Test. 2019;73:214–21. doi:10.1016/j.polymertesting.2018.11.028.
17. Jiang LP, He CX, Fu JJ, Chen D. Wear behavior of wood plastic composites in alternate simulated sea water and acid rain corrosion conditions. Polym Test. 2017;63:236–43.
18. Ratanawilai T, Taneerat K. Alternative polymeric matrices for wood-plastic composites: effects on mechanical properties and resistance to natural weathering. Constr Bulid Mater. 2018;172:349–57.
19. Vedrtnam A, Kumar S, Chaturvedi S. Experimental study on mechanical behavior, biodegradability, and resistance to natural weathering and ultraviolet radiation of wood-plastic composites. Compos Part B. 2019;176:107282. doi:10.1016/j.compositesb.2019.107282.
20. Yu K, Tan X, Hu Y, Chen FW, Li SJ. Microstructure effects on the electrochemical corrosion properties of Mg-4.1%Ga-2.2%Hg alloy as the anode for seawater-activated batteries. Corros Sci. 2011;53:2035–40.
21. Rouhou MC, Abdelmoumen S, Thomas S, Attia H, Ghorbel D. Use of green chemistry methods in the extraction of dietary fibers from cactus rackets (*Opuntia ficus indica*): structural and microstructural studies. Int J Biol Macromol. 2018;116:901–10. doi:10.1016/j.ijbiomac.2018.05.090.
22. Zhu BH, He CX, Shi F, Wang XH, Shi JM, Chen Y. Research progress of plant husk fibers reinforced plastic based composites. Eng Plast Appl. 2016;44(7):142–6 (In Chinese).
23. Li YY, Liu F, Song GS, Han QH. Study on separation of chestnut shell lignin by alkali method. Hubei Agric Sci. 2006;45(6):817–9 (In Chinese).

24. Wang L, He CX, Yang XX. Effects of pretreatment on the soil aging behavior of rice husk fibers/polyvinylchloride composites. BioResources. 2019;14(1):59–69.
25. Badji C, Soccalingame L, Garay H, Bergeret A, Bénézet JC. Influence of weathering on visual and surface aspect of wood plastic composites: correlation approach with mechanical properties and microstructure. Polym Degrad Stabil. 2017;137:162–72. doi:10.1016/j.polymdegradstab.2017.01.010.
26. Matuana LM, Kamdem DP, Zhang J. Photoaging and stabilization of rigid PVC/wood-fiber composites. J Appl Poly Sci. 2001;80(11):1943–50.
27. Shebani AN, Van RAJ, Meinckens M. The effect of wood species on the mechanical and thermal properties of wood-LLDPE composites. J Compos Mater. 2009;43:1305–18.
28. Zhou YH, Fan MZ, Chen LL. Interface and bonding mechanisms of plant fibre composites: an overview. Compos Part B. 2016;101:31–45.
29. Tang FP. Distribution pattern of photodecomposition-oxidation reaction of thick polyvinyl chloride samples—I. Natural climate aging. J Polym Mater. 1989;2:63–8.
30. Matuanaa LM, Jin S, Stark NM. Ultraviolet weathering of HDPE/wood-flour composites coextruded with a clear HDPE cap layer. Polym Degrad Stabil. 2011;96:97–106.